


RESEARCH ARTICLE

Open Access



Effect of Hashimoto's thyroiditis on the dual-energy CT quantitative parameters and performance in diagnosing metastatic cervical lymph nodes in patients with papillary thyroid cancer

Di Geng^{1†}, Yan Zhou^{1†}, Ting Shang^{1,2†}, Guo-Yi Su¹, Shu-shen Lin³, Yan Si⁴, Fei-Yun Wu^{1*}  and Xiao-Quan Xu^{1*}

Abstract

Background To evaluate the effect of Hashimoto's thyroiditis (HT) on dual-energy computed tomography (DECT) quantitative parameters of cervical lymph nodes (LNs) in patients with papillary thyroid cancer (PTC), and its effect on the diagnostic performance and threshold of DECT in preoperatively identifying metastatic cervical LNs.

Methods A total of 479 LNs from 233 PTC patients were classified into four groups: HT+/LN+, HT+/LN-, HT-/LN+ and HT-/LN- group. DECT quantitative parameters including iodine concentration (IC), normalized IC (NIC), effective atomic number (Z_{eff}), and slope of the spectral Hounsfield unit curve (λ_{HU}) in the arterial phase (AP) and venous phase were compared. Receiver operating characteristic curve analyses were performed to evaluate DECT parameters' diagnostic performance in differentiating metastatic from nonmetastatic LNs in the HT- and HT+ groups.

Results The HT+/LN+ group exhibited lower values of DECT parameters than the HT-/LN+ group (all $p < 0.05$). Conversely, the HT+/LN- group exhibited higher values of DECT parameters than the HT-/LN- group (all $p < 0.05$). In the HT+ group, if an AP-IC of 1.850 mg/mL was used as the threshold value, then the optimal diagnostic performance (area under the curve, 0.757; sensitivity, 69.4%; specificity, 71.0%) could be obtained. The optimal threshold value of AP-IC in the HT- group was 2.050 mg/mL. In contrast, in the HT- group, AP-NIC demonstrated the highest area under the curve of 0.988, when an optimal threshold of 0.243 was used. The optimal threshold value of AP-NIC was 0.188 in the HT+ group.

[†]Di Geng, Yan Zhou and Ting Shang contributed equally to this work.

*Correspondence:

Fei-Yun Wu

wfy_njmu@163.com

Xiao-Quan Xu

xiaoquanxu_1987@163.com

Full list of author information is available at the end of the article



© The Author(s) 2024. **Open Access** This article is licensed under a Creative Commons Attribution 4.0 International License, which permits use, sharing, adaptation, distribution and reproduction in any medium or format, as long as you give appropriate credit to the original author(s) and the source, provide a link to the Creative Commons licence, and indicate if changes were made. The images or other third party material in this article are included in the article's Creative Commons licence, unless indicated otherwise in a credit line to the material. If material is not included in the article's Creative Commons licence and your intended use is not permitted by statutory regulation or exceeds the permitted use, you will need to obtain permission directly from the copyright holder. To view a copy of this licence, visit <http://creativecommons.org/licenses/by/4.0/>. The Creative Commons Public Domain Dedication waiver (<http://creativecommons.org/publicdomain/zero/1.0/>) applies to the data made available in this article, unless otherwise stated in a credit line to the data.

Conclusions HT affected DECT quantitative parameters of LNs and subsequent the diagnostic thresholds. When using DECT to diagnose metastatic LNs in patients with PTC, whether HT is coexistent should be clarified considering the different diagnostic thresholds.

Keywords Papillary thyroid cancer, Thyroiditis, Lymphatic metastasis, Multidetector computed tomography

Introduction

Papillary thyroid cancer (PTC) accounts for up to 90% of the malignant tumors in the thyroid [1]. Cervical lymph node (LN) metastasis is highly associated with a poor prognosis of PTC [2]. Therefore, accurate preoperative identification of metastatic LNs is important for establishing the individual treatment plan for patients with PTC. Ultrasonography (US) is usually first suggested for evaluating the status of cervical LNs in patients with PTC in clinical practice [2]. However, US is operator dependent, and it is limited in the evaluation of central LNs because of the gas interference in the trachea and esophagus and the shield of the sternum and clavicle [3, 4]. Although administration of iodine-containing contrast can potentially suppress thyroidal radioactive iodine uptake and subsequently postpone radioiodine therapy [5], contrast-enhanced computed tomography (CT) can provide more detailed anatomic information, and previous studies have reported that CT combined with US can improve the sensitivity in diagnosing metastatic LNs [4, 6]. However, it is typical to assess the morphology-based imaging features of these two modalities for subsequent differential diagnosis, which is subjective. An objective approach that can provide quantitative biological information is needed in the clinical setting.

Dual-energy CT (DECT) is an advanced imaging technique that allows high- and low-energy image acquisitions using two different X-ray tube voltages, subsequently generating a variety of material decomposition images [7]. By reconstructing multiparameter images, DECT could provide more quantitative information by calculating parameters including iodine concentration (IC), effective atomic number (Z_{eff}) and slope of the spectral Hounsfield unit curve (λ_{HU}), which offers a noninvasive alternative to tissue characterization [8]. Previously, Liu X et al. reported that λ_{HU} , normalized IC (NIC), and normalized Z_{eff} derived from DECT of cervical metastatic LNs were higher than those of nonmetastatic LNs [9]. DECT may be a promising approach for diagnosing the metastatic LNs in patients with PTC [9].

Recently, the coexistence of Hashimoto's thyroiditis (HT) in patients with PTC has attracted increasing attention [10]. Moreover, previous studies have proved that the incidence of PTC is higher in patients with HT [11, 12]. HT is characterized by the lymphocytic infiltration caused by relevant autoantibodies [13]. A similar immune response can also occur in the thyroid-draining cervical LNs, subsequently leading to reactive lymphadenopathy.

Concerning location, enlarged infrathyroidal and/or pretracheal reactive LNs are commonly observed in patients with HT [14, 15]. Meanwhile, in clinical practice, we also find that reactive hyperplastic LNs in patients with HT also often display a marked enhancement on CT images, which increases the difficulty in differentiating metastatic from nonmetastatic LNs. However, to the best of our knowledge, to date, there is still a dearth of studies focusing on the effect of HT on the DECT parameters and subsequent performance or threshold in diagnosing metastatic LNs.

Therefore, the purpose of our study was to: (1) examine the effect of HT on the DECT-derived quantitative parameters of cervical metastatic and nonmetastatic LNs and (2) evaluate the effect of HT on the performance and threshold of DECT-derived quantitative parameters in preoperatively diagnosing metastatic cervical LNs in patients with PTC.

Materials and methods

Study population

This retrospective study was approved by the institutional ethics committee (2022-SREA-035), and the requirement for written informed consent was waived. Between June 2017 and June 2022, a total of 2,263 consecutive patients with suspected PTC underwent preoperative DECT scans for pretreatment evaluation. We retrospectively included the study population according to the following criteria: (1) confirmation of PTC by histopathology, (2) cervical LN dissection was performed and the pathological result was obtained, (3) DECT scans were examined within 1 month before surgery and lymph nodes with maximum short axis diameters ≥ 5 mm were found on images, (4) no history of radiotherapy or chemotherapy before surgery, (5) no history of other malignancies, and (6) adequate DECT image quality for subsequent analyses. Diagnosis of coexistent HT was established according to the method proposed in a previous study [16]. Specifically, PTC patients were considered to have coexistent HT if "Hashimoto's thyroiditis," "lymphocytic thyroiditis," or "chronic lymphocytic thyroiditis" was reported in postoperative pathology. Finally, 233 patients (including 124 patients with HT) were included in our study. All patients enrolled were euthyroid. In addition, urinary iodine concentrations were measured in 87 of 233 patients. The median urinary iodine level was 235.8 $\mu\text{g/L}$ (reference range, 100.0–300.0 $\mu\text{g/L}$). Detailed patient characteristics are presented in Table 1.

Table 1 Demographics and lymph nodes distribution of PTC patients with HT and without HT.

Variables	With HT	With-out HT	<i>p</i> value
Patients	124	109	
Sex			0.002
Male	29	46	
Female	95	63	
Age (years)			0.002
Median (interquartile range)	32.0 (28.0–40.0)	37.0 (31.0–44.5)	
LN distribution	255	224	0.001
Metastatic	62	93	
Nonmetastatic	193	131	
Lateral LN	174	166	0.118
Metastatic	25	35	
Nonmetastatic	149	131	

Note: PTC, papillary thyroid cancer; HT, Hashimoto's thyroiditis; LN, lymph nodes

p values indicate the comparisons among sex, age, and numbers of metastatic and nonmetastatic LNs in the cervical and lateral cervical regions between patients with HT and without HT in column order

DECT examination

Imaging acquisition was performed using a third-generation dual-source DECT scanner (Somatom Force; Siemens Healthcare). Scans ranged from the skull base to the upper margin of the aortic arch. Detailed scan parameters were as follows: tube A voltage, 80 kV; tube B voltage, Sn150 kV; detector configuration, 128×0.6 mm; rotation time, 0.5 s; pitch, 0.7; and matrix, 256×256. Automatic attenuation-based tube current modulation (CARE Dose 4D; Siemens Healthcare) combined with an iterative reconstruction algorithm (ADMIRE, Siemens Healthcare, Strength Level 3) was used to reduce the radiation dose. For contrast-enhanced scan, 75 mL of contrast agent (iopromide; Bayer Healthcare) was injected into the elbow vein at a flow of 3.5 mL/s using an automated high-pressure syringe. Image acquisition of the arterial phase (AP) and venous phase (VP) started at 25 and 50 s after contrast agent injection, respectively.

LN histopathologic marking on DECT images

The LN levels were recorded according to the American Joint Committee on Cancer cervical regional lymph node level system. The status of LNs was defined according to surgical pathology reports of neck dissection. LN histopathologic marking on DECT images was in accordance with one method proposed in a previous study [17]. If all the LNs in one level were histologically proven to be metastatic, then the LNs visible on DECT images at this level were all assigned as metastatic LNs. If all the LNs in one level were histologically proven to be nonmetastatic, then the LNs visible on DECT images at this level were all assigned as nonmetastatic LNs. If one level contained

both metastatic and nonmetastatic LNs, then all the LNs visible on DECT images at this level were excluded from further analyses.

Finally, a total of 479 cervical LNs were enrolled and divided into four groups (1) HT+/LN+group (metastatic LNs in PTC patients with HT, *n*=63), (2) HT+/LN−group (nonmetastatic LNs in PTC patients with HT, *n*=193), (3) HT−/LN+group (metastatic LNs in PTC patients without HT, *n*=93), and (4) HT−/LN−group (nonmetastatic LNs in PTC patients without HT, *n*=131).

Image analysis

Iodine maps, Z_{eff} maps, and virtual monochromatic images were reconstructed using commercially available software (*syngo.via*, version VB10B; Siemens Healthcare). A circular region of interest was drawn manually on the axial slice showing the maximum short axis diameter of LN, avoiding vessels and necrotic areas. After the region of interest was placed, IC and Z_{eff} could be obtained automatically. Normalized IC was calculated as follows: $IC = IC_{\text{LN}}/IC_{\text{CCA}}$, where IC_{LN} is the IC of LN and IC_{CCA} is the IC of the common carotid artery at the same level as the LN. Energy spectrum curves at 40 to 190 keV energy levels were plotted. The slope of the Hounsfield unit curve (λ_{HU}) was calculated as follows: $[\lambda_{\text{HU}} = (40 \text{ keV}_{\text{HU}} - 70 \text{ keV}_{\text{HU}})/30 \text{ keV}]$, where 40 keV_{HU} and 70 keV_{HU} are the HU values of the 40- and 70-keV monochromatic images, respectively [9]. Measurements were repeated two times, and the average values were calculated for subsequent statistical analyses.

Statistical analyses

The Kolmogorov–Smirnov test was used to evaluate whether the data were normally distributed or not. Because of the non-normal distribution of the parameters in the four groups, all data were presented as median (interquartile range). The Kruskal–Wallis test with subsequent post-hoc pairwise was then used to compare the differences of continuous variables among the four groups. Receiver operating characteristic curves together with the area under the curve (AUC), sensitivity and specificity were used to evaluate the diagnostic performance and threshold of DECT-derived quantitative parameters. Statistical analyses were performed using SPSS software (version 26.0; IBM). All *p* values were two-sided with significance at less than 0.05.

Results

Effect of HT on DECT-derived quantitative parameters of cervical metastatic and nonmetastatic LNs in PTC patients

DECT quantitative parameters of the four groups are summarized in Table 2 (Fig. 1a–h). Significant differences were observed in all DECT quantitative parameters in both the AP and VP among the four groups (all *p*<0.001;

Table 2 Comparison of quantitative dual-energy CT parameters between metastatic and nonmetastatic lymph nodes in PTC patients with and without HT

	HT+/LN+ (n=62)	HT+/LN- (n=193)	HT-/LN+ (n=93)	HT-/LN- (n=131)	p value	p ^a value	p ^b value	p ^c value	p ^d value
Arterial phase									
IC (mg/mL)	2.200 (1.600–2.700)	1.500 (1.100–2.000)	4.000 (3.000–5.000)	1.100 (0.800–1.500)	<0.001	<0.001	<0.001	<0.001	<0.001
NIC	0.251 (0.193–0.306)	0.169 (0.128–0.219)	0.432 (0.335–0.512)	0.125 (0.091–0.160)	<0.001	<0.001	<0.001	<0.001	<0.001
Z _{eff}	8.700 (8.400–9.000)	8.300 (8.150–8.600)	9.400 (9.050–9.700)	8.100 (7.900–8.300)	<0.001	<0.001	<0.001	<0.001	<0.001
λ _{HU}	4.454 (3.515–5.457)	3.086 (2.289–4.041)	7.573 (5.518–9.867)	2.408 (1.641–3.204)	<0.001	<0.001	<0.001	<0.001	<0.001
Venous phase									
IC (mg/mL)	2.300 (1.775–3.400)	2.100 (1.700–2.400)	3.200 (2.600–3.900)	1.800 (1.400–2.100)	<0.001	0.018	<0.001	<0.001	0.001
NIC	0.488 (0.385–0.658)	0.447 (0.364–0.525)	0.698 (0.570–0.837)	0.395 (0.326–0.468)	<0.001	0.167	<0.001	<0.001	0.004
Z _{eff}	8.700 (8.400–9.200)	8.600 (8.400–8.750)	9.100 (8.800–9.450)	8.500 (8.300–8.600)	<0.001	0.045	<0.001	<0.001	0.001
λ _{HU}	4.760 (3.856–6.708)	4.121 (3.434–5.056)	6.166 (4.795–7.828)	3.718 (2.979–4.264)	<0.001	0.005	<0.001	0.003	0.001

Note: PTC, papillary thyroid cancer; HT, Hashimoto's thyroiditis; HT+, PTC with HT; HT-, PTC without HT; LN+, metastatic lymph nodes; LN-, nonmetastatic LNs; IC, iodine concentration; NIC, normalized IC; Z_{eff}, effective atomic number; λ_{HU}, slope of the spectral Hounsfield unit curve

p^a value, HT+/LN+ vs. HT+/LN-; p^b value, HT-/LN+ vs. HT-/LN-; p^c value, HT+/LN+ vs. HT-/LN+; p^d value, HT+/LN- vs. HT-/LN-.

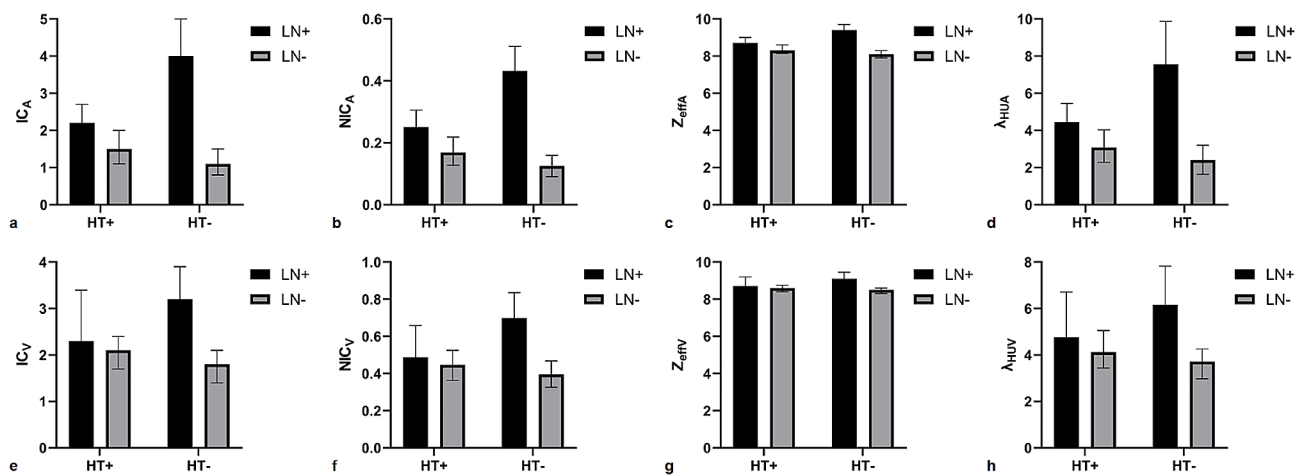


Fig. 1 IC_A/IC_V (a, e), NIC_A/NIC_V (b, f), Z_{effA}/Z_{effV} (c, g), and λ_{HUA}/λ_{HUV} (d, h) of metastatic and nonmetastatic lymph nodes in PTC patients with HT and without HT. All p values except NIC_V between LN+ and LN- in HT+ patients are greater than 0.05. PTC, papillary thyroid cancer; HT, Hashimoto's thyroiditis; HT+, PTC with HT; HT-, PTC without HT; LN+, metastatic lymph nodes; LN-, nonmetastatic LNs; IC_A/IC_V, iodine concentration in arterial/venous phase; NIC_A/NIC_V, normalized IC_A/IC_V; Z_{effA}/Z_{effV}, effective atomic number in arterial/venous phase; and λ_{HUA}/λ_{HUV}, slope of the spectral Hounsfield unit curve in arterial/venous phase

Table 2). The values of all DECT quantitative parameters measured in the HT+/LN+ group were significantly lower than those in the HT-/LN+ group, whereas they were significantly higher in the HT+/LN- group than in the HT-/LN- group (all *p* < 0.05; Table 2). Representative cases are shown in Figs. 2 and 3.

Effect of HT on the performance or threshold of DECT in preoperatively diagnosing metastatic cervical LNs in PTC patients

The HT+/LN+ group exhibited significantly higher NIC in the AP and higher IC, Z_{eff} and λ_{HU} in both the AP and VP than the HT+/LN- group (all *p* < 0.05; Table 2). The values of all DECT parameters measured in both the AP and VP were significantly higher in the HT-/LN+ group than those in the HT-/LN- group (all *p* < 0.001; Table 2).

The diagnostic performance, sensitivity, and specificity of each DECT parameter in differentiating metastatic from nonmetastatic LNs in both the HT+ and HT- groups are listed in Table 3. The thresholds of these DECT parameters differed in the HT+ and HT- PTC patients, and the AUCs were all greater than 0.600 (Table 3; Fig. 4). In the HT+ group, the AUCs of DECT parameters in the AP were greater than 0.700, which indicated higher diagnostic value. In the HT- group, the AUCs of all DECT parameters in the AP and VP were greater than 0.900, which indicated excellent performance.

In the HT+ group, if an AP-IC of 1.850 mg/mL was used as a threshold value, then optimal diagnostic performance (AUC, 0.757; sensitivity, 69.4%; and specificity, 71.0%) could be obtained (Table 3; Fig. 4a). In contrast, in

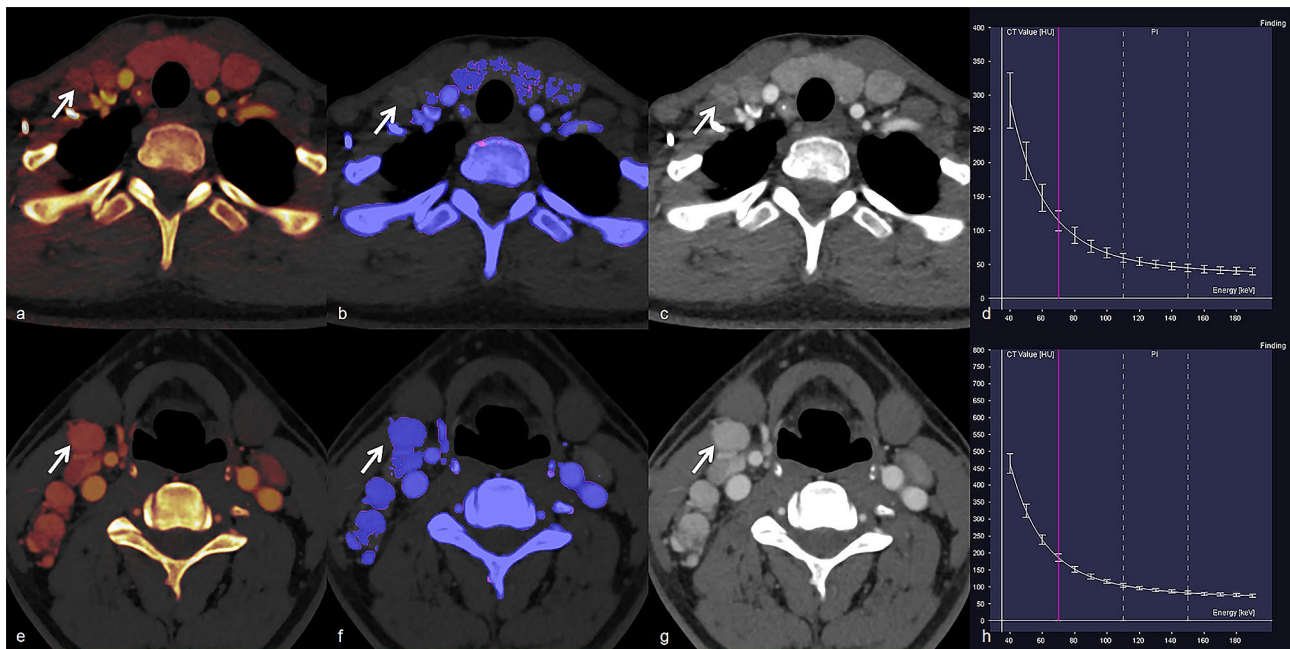


Fig. 2 Representative images and energy spectrum curves of metastatic lateral lymph nodes in PTC patients with HT (a–d) and without HT (e–h). Metastatic LNs in PTC patients with HT demonstrated lower IC (3.000 vs. 6.300 mg/mL), NIC (0.248 vs. 0.670), Z_{eff} (9.000 vs. 10.200), and λ_{HU} (5.924 vs. 11.313) than those in PTC patients without HT in arterial phase. PTC, papillary thyroid cancer; HT, Hashimoto's thyroiditis; LN, lymph node; IC, iodine concentration; NIC, normalized IC; Z_{eff} , effective atomic number; and λ_{HU} , slope of the spectral Hounsfield unit curve

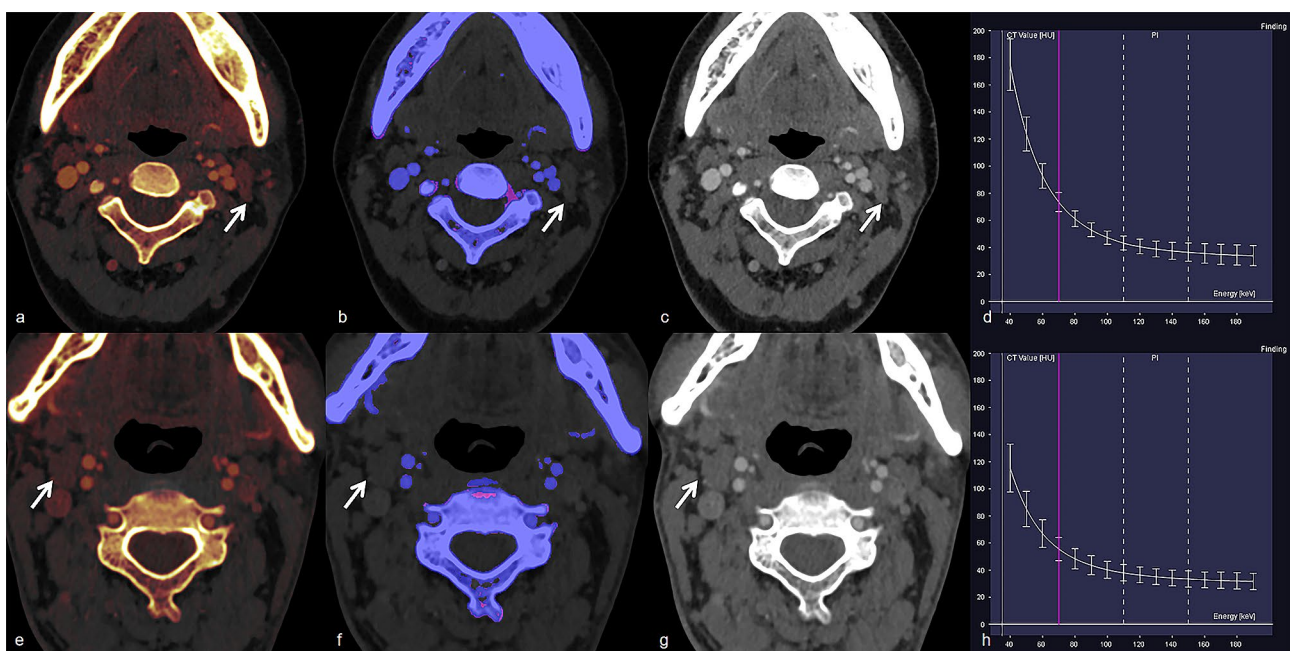


Fig. 3 Representative images and energy spectrum curves of nonmetastatic lateral lymph nodes in PTC patients with HT (a–d) and without HT (e–h). Nonmetastatic LNs in PTC patient with HT demonstrated higher IC (1.700 vs. 0.900 mg/mL), NIC (0.210 vs. 0.134), Z_{eff} (8.400 vs. 8.000), and λ_{HU} (3.381 vs. 1.989) than those in PTC patients without HT in arterial phase. PTC, papillary thyroid cancer; HT, Hashimoto's thyroiditis; LN, lymph node; IC, iodine concentration; NIC, normalized IC; Z_{eff} , effective atomic number; and λ_{HU} , slope of the spectral Hounsfield unit curve

the HT–group, the optimal threshold value of AP-IC was 2.050 mg/mL (Table 3; Fig. 4b).

However, in the HT–group, AP-NIC demonstrated the highest AUC of 0.988, sensitivity of 91.4%, and specificity

of 99.2% when an optimal threshold of 0.243 was used (Table 3; Fig. 4b). In contrast, in the HT+group, the optimal threshold value of AP-NIC was 0.188 (Table 3; Fig. 4a).

Table 3 Diagnostic performance of dual-energy CT parameters in differentiating metastatic from nonmetastatic lymph nodes in PTC patients with and without HT

	Threshold	AUC	Sensitivity	Specificity
HT+/LN+ vs. HT+/LN-				
IC _A (mg/mL)	1.850	0.757	0.694	0.710
NIC _A	0.188	0.749	0.823	0.611
Z _{effA}	8.350	0.753	0.806	0.549
λ _{HUA}	3.798	0.726	0.710	0.715
IC _V (mg/mL)	2.950	0.630	0.371	0.917
Z _{effV}	8.950	0.616	0.371	0.891
λ _{HUV}	6.116	0.651	0.371	0.948
HT-/LN+ vs. HT-/LN-				
IC _A (mg/mL)	2.050	0.983	0.925	0.977
NIC _A	0.243	0.988	0.914	0.992
Z _{effA}	8.650	0.980	0.903	0.985
λ _{HUA}	4.310	0.971	0.882	0.969
IC _V (mg/mL)	2.550	0.929	0.785	0.947
NIC _V	0.576	0.932	0.753	0.962
Z _{effV}	8.750	0.920	0.806	0.901
λ _{HUV}	4.601	0.903	0.828	0.878

Note: PTC, papillary thyroid cancer; HT, Hashimoto's thyroiditis; HT+, PTC with HT; HT-, PTC without HT; LN+, metastatic lymph nodes; LN-, nonmetastatic LNs; IC_A/IC_V, iodine concentration in arterial/venous phase; NIC_A/NIC_V, normalized IC_A/IC_V; Z_{effA}/Z_{effV}, effective atomic number in arterial/venous phase; λ_{HUA}/λ_{HUV}, slope of the spectral Hounsfield unit curve in arterial/venous phase. AUC, area under the curve

Threshold IC_A/IC_V are represented as mg/mL

Subgroup analysis of the effect of HT on DECT-derived quantitative parameters of lateral cervical metastatic and nonmetastatic LNs

We further compared DECT quantitative parameters of lateral LNs among the four groups (Table 4; Fig. 5a–h).

Similarly, the values of the DECT quantitative parameters of the lateral HT+/LN+ group were significantly lower than those of the lateral HT-/LN+ group, whereas the values of the parameters of the lateral HT+/LN- group were significantly higher than those of the parameters of the lateral HT-/LN- group (all $p < 0.05$; Table 4).

Subgroup analysis of the effect of HT on the performance of DECT in preoperatively diagnosing lateral cervical metastatic LNs.

The lateral HT+/LN- group exhibited significantly lower values of all DECT quantitative parameters than the lateral HT+/LN+ group (all $p < 0.05$; Table 4), except λ_{HU} in the VP ($p = 0.060$). In addition, the values of all DECT quantitative parameters measured in both the AP and VP of the lateral HT-/LN+ group were significantly higher than those of the lateral HT-/LN- group (all $p < 0.001$; Table 4).

Diagnostic performance, sensitivity and specificity of each DECT quantitative parameter in differentiating lateral metastatic from nonmetastatic LNs in both the HT+ and HT- groups are presented in Table 5. The thresholds of these DECT parameters differed between the HT+ and HT- patients, with all AUCs greater than 0.600 (Table 5; Fig. 6). In the HT+ group, the AUCs of DECT parameters in the AP were greater than 0.700, indicating higher diagnostic ability. In the HT- group, all DECT parameters in the AP and VP indicated excellent performance with AUCs greater than 0.900.

Receiver operating characteristic curve analyses demonstrated that the AP-λ_{HU} had optimal diagnostic performance (AUC, 0.800; sensitivity, 79.2%; specificity, 77.1%) for diagnosing lateral metastatic LNs in the HT+ group

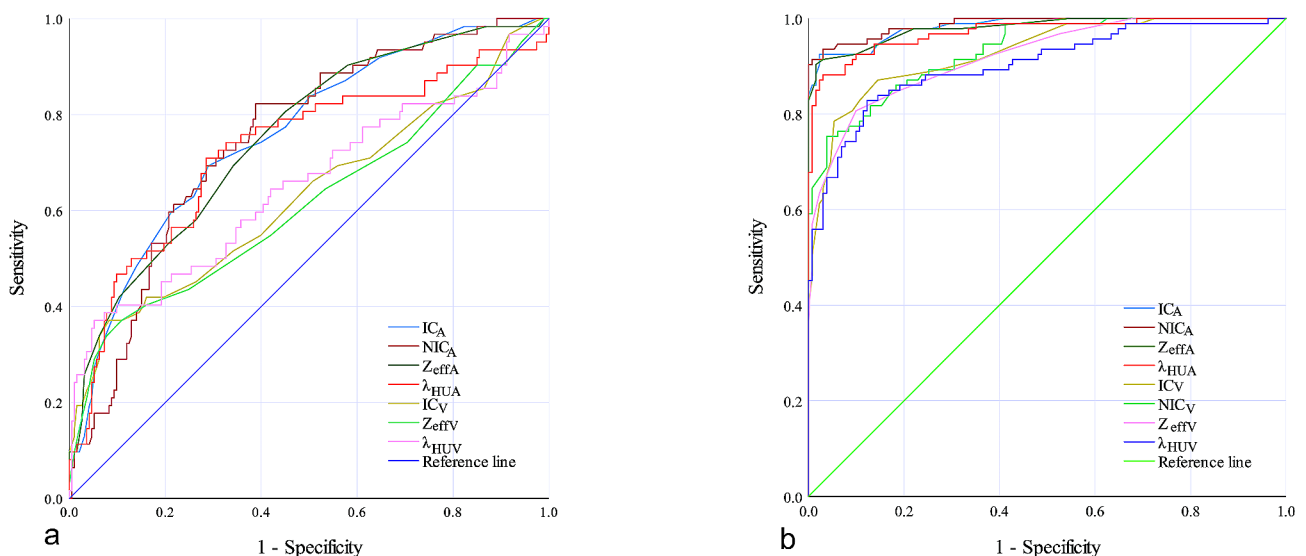


Fig. 4 ROC curves using IC_A/IC_V, NIC_A/NIC_V, Z_{effA}/Z_{effV} and λ_{HUA}/λ_{HUV} in differentiating metastatic and nonmetastatic lymph nodes in PTC patients with HT (a) and without HT (b). PTC, papillary thyroid cancer; HT, Hashimoto's thyroiditis; IC_A/IC_V, iodine concentration in arterial/venous phase; NIC_A/NIC_V, normalized IC_A/IC_V; Z_{effA}/Z_{effV}, effective atomic number in arterial/venous phase; λ_{HUA}/λ_{HUV}, slope of the spectral Hounsfield unit curve in arterial/venous phase; and ROC, receiver operating characteristic

Table 4 Comparison of quantitative dual-energy CT parameters between lateral metastatic and nonmetastatic lymph nodes in PTC patients with and without HT

	HT+/LLN+ (n=24)	HT+/LLN- (n=149)	HT-/LLN+ (n=35)	HT-/LLN- (n=131)	p value	p ^a value	p ^b value	p ^c value	p ^d value
Arterial phase									
IC (mg/mL)	1.950 (1.600–2.500)	1.300 (1.100–1.800)	4.700 (3.500–5.300)	1.100 (0.800–1.500)	<0.001	<0.001	<0.001	0.022	<0.001
NIC	0.243 (0.193–0.274)	0.157 (0.122–0.202)	0.467 (0.357–0.554)	0.125 (0.091–0.160)	<0.001	<0.001	<0.001	0.021	<0.001
Z _{eff}	8.500 (8.400–8.875)	8.200 (8.100–8.400)	9.600 (9.300–9.800)	8.100 (7.900–8.300)	<0.001	<0.001	<0.001	0.022	<0.001
λ _{HU}	3.968 (3.447–5.390)	2.757 (2.104–3.560)	9.807(6.403–10.395)	2.408 (1.641–3.204)	<0.001	<0.001	<0.001	0.029	0.005
Venous phase									
IC (mg/mL)	2.250 (2.025–3.375)	2.100 (1.700–2.300)	3.000 (2.500–4.000)	1.800 (1.400–2.100)	<0.001	0.013	<0.001	0.018	<0.001
NIC	0.529 (0.412–0.695)	0.449 (0.376–0.517)	0.703 (0.591–0.840)	0.395 (0.326–0.468)	<0.001	0.025	<0.001	0.009	<0.001
Z _{eff}	8.700 (8.500–9.200)	8.600 (8.400–8.700)	9.100 (8.800–9.500)	8.500 (8.300–8.600)	<0.001	0.040	<0.001	0.007	<0.001
λ _{HU}	4.675 (3.682–6.652)	4.100 (3.489–4.902)	5.826 (4.748–7.902)	3.718 (2.979–4.264)	<0.001	0.060	<0.001	0.011	<0.001

Note: PTC, papillary thyroid cancer; HT, Hashimoto's thyroiditis; HT+, PTC with HT; HT-, PTC without HT; LLN+, metastatic lateral lymph nodes; LLN-, nonmetastatic LLNs; IC, iodine concentration; NIC, normalized IC; Z_{eff}, effective atomic number; λ_{HU}, slope of the spectral Hounsfield unit curve

p^a value, HT+/LLN+ vs. HT+/LLN-; p^b value, HT-/LLN+ vs. HT-/LLN-; p^c value, HT+/LLN+ vs. HT-/LLN+; p^d value, HT+/LLN- vs. HT-/LLN-.

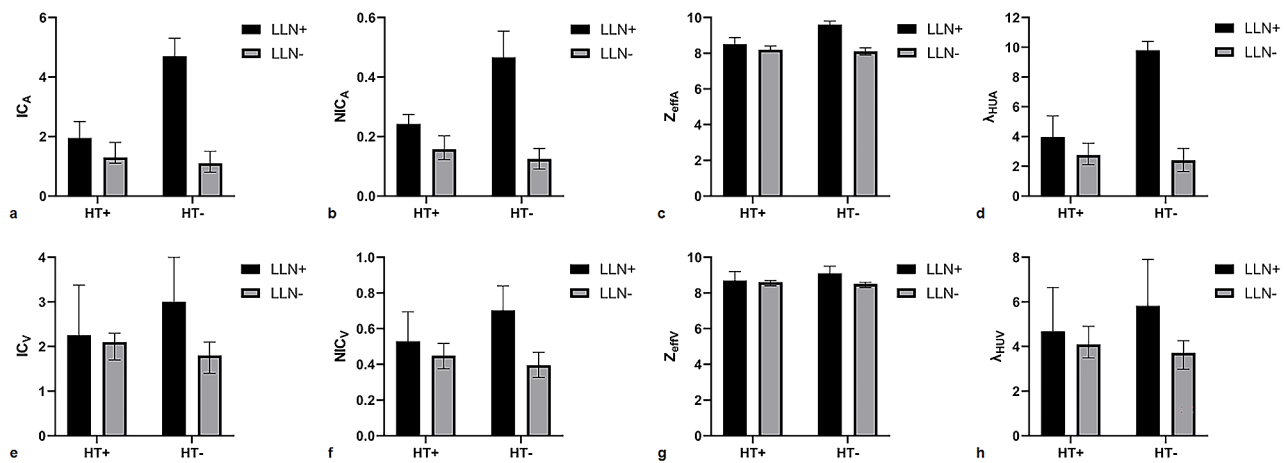


Fig. 5 IC_A/IC_V (a, e), NIC_A/NIC_V (b, f), Z_{effA}/Z_{effV} (c, g), and λ_{HUA}/λ_{HUV} (d, h) of metastatic and nonmetastatic lymph nodes in PTC patients with HT and without HT. All p values except λ_{HUV} between LN+ and LN- in HT+ patients are greater than 0.05. PTC, papillary thyroid cancer; HT, Hashimoto's thyroiditis; HT+, PTC with HT; HT-, PTC without HT; LN+, metastatic lymph nodes; LN-, nonmetastatic LLNs. IC_A/IC_V, iodine concentration in arterial/venous phase; NIC_A/NIC_V, normalized IC_A/IC_V; Z_{effA}/Z_{effV}, effective atomic number in arterial/venous phase; and λ_{HUA}/λ_{HUV}, slope of the spectral Hounsfield unit curve in arterial/venous phase

when 3.398 was used as the threshold value (Table 5; Fig. 6a). In contrast, in the HT-PTC group, the optimal threshold value of AP-λ_{HU} was 4.310 (Table 5; Fig. 6b).

However, in the HT-group, AP-NIC showed optimal diagnostic performance (AUC, 0.989; sensitivity, 97.1%; and specificity, 96.9%) when 0.226 was used as the threshold value (Table 5; Fig. 6b). In contrast, in the HT+group, the optimal threshold of AP-NIC was 0.193 (Table 5; Fig. 6a).

Discussion

In the present study, we observed that the coexistence of HT may influence the DECT quantitative parameters of cervical LNs. Metastatic LNs in the HT+group exhibited lower values of DECT quantitative parameters than those in the HT-group, whereas nonmetastatic LNs in the

HT+group exhibited higher values of DECT quantitative parameters. Furthermore, the optimal threshold values of DECT quantitative parameters for diagnosing metastatic cervical LNs differed between the HT+ and HT-groups. These findings remained consistent in the subgroup analysis of lateral cervical LNs. To the best of our knowledge, our study was the first to evaluate the effect of HT on DECT quantitative parameters themselves, their performance and thresholds in preoperatively diagnosing metastatic cervical LNs in patients with PTC.

HT is an autoimmune disease characterized by lymphocyte and macrophage infiltration within and surrounding the tumors, which could interfere with the tumor microenvironment to improve antitumor immune responses [18, 19]. The presence of inflammatory and immune responses may be combined to result in a lower

Table 5 Diagnostic performance of dual-energy CT parameters in differentiating lateral metastatic from nonmetastatic lymph nodes in PTC patients with and without HT

	Threshold	AUC	Sensitivity	Specificity
HT+/LLN+ vs. HT+/LLN-				
IC _A (mg/mL)	1.550	0.780	0.792	0.638
NIC _A	0.193	0.780	0.792	0.698
Z _{effA}	8.350	0.780	0.792	0.638
λ _{HUA}	3.398	0.800	0.792	0.711
IC _V (mg/mL)	2.950	0.668	0.417	0.966
NIC _V	0.523	0.649	0.542	0.765
Z _{effV}	8.950	0.644	0.417	0.946
HT-/LLN+ vs. HT-/LLN-				
IC _A (mg/mL)	2.050	0.980	0.914	0.977
NIC _A	0.226	0.989	0.971	0.969
Z _{effA}	8.550	0.978	0.914	0.969
λ _{HUA}	4.310	0.971	0.914	0.969
IC _V (mg/mL)	2.250	0.926	0.886	0.855
NIC _V	0.577	0.952	0.829	0.962
Z _{effV}	8.750	0.922	0.829	0.901
λ _{HUV}	4.601	0.914	0.886	0.878

Note: PTC, papillary thyroid cancer; HT, Hashimoto's thyroiditis; HT+, PTC with HT; HT-, PTC without HT; LLN+, metastatic lateral lymph nodes; LLN-, nonmetastatic LLNs; IC_A/IC_V, iodine concentration in arterial/venous phase; NIC_A/NIC_V, normalized IC_A/IC_V; λ_{HUA}/λ_{HUV}, slope of the spectral Hounsfield unit curve in arterial/venous phase; Z_{effA}/Z_{effV}, effective atomic number in arterial/venous phase. AUC, area under the curve

Threshold IC_A/IC_V are represented as mg/mL

rate of angiolymphatic invasion in the HT+group [16]. As a result, metastatic LNs in the HT+group exhibited lower values of DECT quantitative parameters than those in the HT−group. In addition, previous studies

have reported that the clonal expansion and maturation of autoreactive CD4+T cells, CD8+cytotoxic T cells, and B cells could result in the uncontrolled production of autoantibodies in the central stage of the development of HT, subsequently leading to cervical lymphadenopathy. This situation can increase the misdiagnosis risks of metastatic LNs based on imaging [14, 20]. This may be ascribed to the increased vessel density in reactive inflammatory nonmetastatic LNs in the HT+group [21]. Thus, they would present higher IC, NIC, Z_{eff} and λ_{HU} than nonmetastatic LNs in the HT−group. US is the most common method used for assessing the status of LNs in patients with PTC. The effect of HT on the diagnostic efficacy of US for cervical LNs in PTC patients has also been investigated in a previous study [22]. Tan HL et al. reported that HT can interfere with the evaluation of US by increasing the frequency of fatty hilum absence in benign central LNs, thereby reducing its diagnostic accuracy and increasing the misdiagnosis rate [22]. Therefore, according to our findings, we believe that the LNs of PTC patients with concomitant HT should be thoroughly evaluated by clinicians, wherein DECT could serve as an indispensable adjunct modality.

IC and NIC provide an objective and quantitative assessment of iodine contrast agent uptake, which indirectly reflects the angiogenesis of lesions [23, 24]. Z_{eff} provides information on the elemental composition of materials, whereas λ_{HU} is determined by the physical and chemical nature of tissues [25]. The alterations in IC and NIC will cause differences in the composition and characteristics of tissues, leading to changes in Z_{eff} and λ_{HU}.

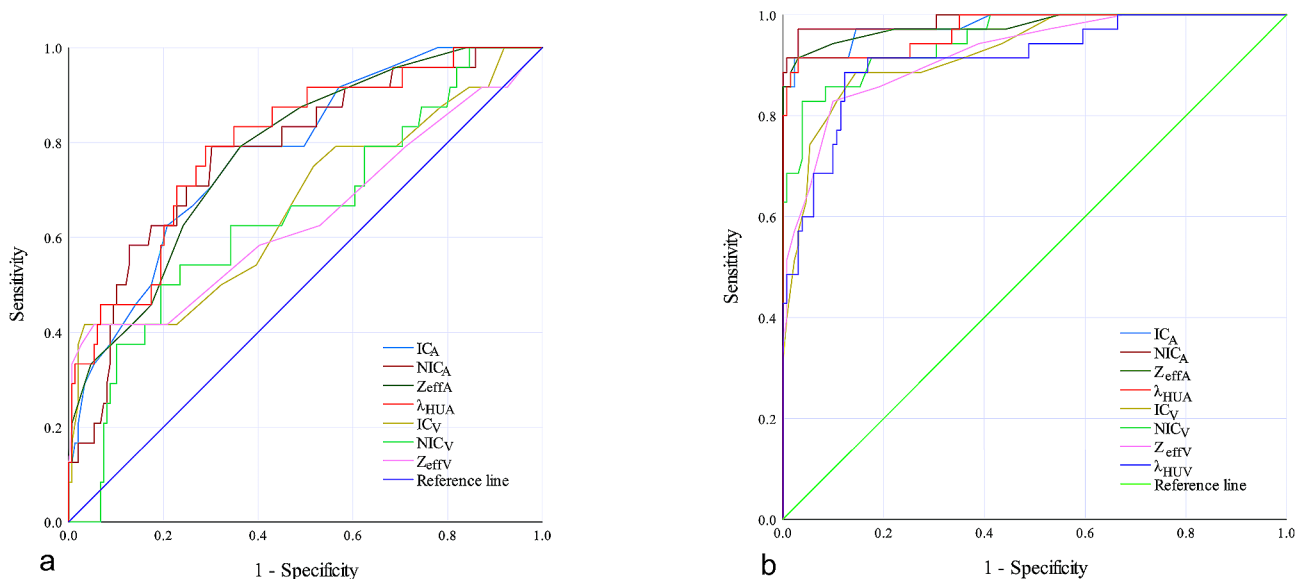


Fig. 6 ROC curves using IC_A/IC_V, NIC_A/NIC_V, Z_{effA}/Z_{effV}, and λ_{HUA}/λ_{HUV} in differentiating lateral metastatic and nonmetastatic lymph nodes in PTC patients with HT (a) and without HT (b). PTC, papillary thyroid cancer; HT, Hashimoto's thyroiditis; IC_A/IC_V, iodine concentration in arterial/venous phase; NIC_A/NIC_V, normalized IC_A/IC_V; Z_{effA}/Z_{effV}, effective atomic number in arterial/venous phase; λ_{HUA}/λ_{HUV}, slope of the spectral Hounsfield unit curve in arterial/venous phase; and ROC, receiver operating characteristic

Our study revealed again that the values of the DECT parameters of the metastatic LNs in both the arterial and venous phases were significantly higher than those of the nonmetastatic LNs, which was in line with the previous studies [9, 26]. This finding may be ascribed to the abundant blood supply in metastatic LNs [27]. However, because of the effect of HT on the DECT parameters themselves, the diagnostic performance and thresholds differed in the HT+ and HT− groups. The findings of the present study suggested that whether HT was coexistent or not should be clarified before imaging diagnosis and that it is crucial during the interpretation of imaging features and parameters.

Lateral LN metastasis was considered as a risk factor for disease recurrence and poor prognosis of PTC [28]. Lateral neck dissection is widely considered a necessary procedure for patients with confirmed lateral metastatic LNs [2]. Therefore, preoperative identification of lateral LN metastasis is essential for PTC patients. Our subgroup analysis of lateral LN confirmed again the potential influence of HT on DECT parameters themselves, their performance, and thresholds and emphasized the importance of clarifying whether HT was coexistent or not beforehand.

There were several limitations in our study. First, this was a retrospective single-center study with inevitable selection bias. Second, the pathological findings of the HT+ and HT− LNs were not studied. Further study corresponding to DECT and pathological findings would be valuable to confirm and explain our results.

Conclusions

Our findings indicated that the presence of coexistent HT affected the DECT quantitative parameters of cervical LNs in patients with PTC. Furthermore, the optimal thresholds of DECT quantitative parameters for diagnosing metastatic LNs in the HT+ and HT− groups may be different. Before diagnosing the metastatic LNs in patients with PTC with reference to the DECT quantitative parameters, whether HT was coexistent should be clarified.

Abbreviations

PTC	Papillary thyroid cancer
LN	Lymph node
US	Ultrasonography
CT	Computed tomography
DECT	Dual-energy computed tomography
IC	Iodine concentration
NIC	Normalized iodine concentration
Z_{eff}	Effective atomic number
λ_{HU}	Slope of the spectral Hounsfield unit curve
AP	Arterial phase
VP	Venous phase
HT	Hashimoto's thyroiditis
AUC	Area under the curve

Acknowledgements

We thank LetPub (www.letpub.com) for its linguistic assistance during the preparation of this manuscript.

Author contributions

DG: Investigation; Data analysis; Methodology; Visualization; Writing-original draft. YZ: Investigation; Data curation; Writing-original draft. TS: Investigation; Data curation; Writing-original draft. GYS: Investigation; Data curation. SSL: Data analysis. YS: Data curation. FYW: Conceptualization; Funding acquisition; Supervision. XQX: Conceptualization; Funding acquisition; Methodology; Supervision; Writing-original draft. All authors: Writing-review & editing.

Funding

This study has received funding by Basic (Natural) Science Foundation of Education Department of Jiangsu Province (22KJB320005 to Xiao-Quan Xu), Natural Science Foundation of China (82171928 to Fei-Yun Wu), Natural Science Foundation of Jiangsu Province (BK20201494 to Fei-Yun Wu) and Jiangsu Province Capability Improvement Project through Science, Technology and Education (JSDW202243 to Fei-Yun Wu).

Data availability

The datasets used and/or analysed during the current study are available from the corresponding author on reasonable request.

Declarations

Ethics approval and consent to participate

This study was approved by the institutional review board of our hospital. Written informed consent was waived due to the retrospective nature of our study.

Consent for publication

All authors read and approved the final manuscript.

Competing interests

All authors declare that they have no competing interests.

Author details

¹Department of Radiology, The First Affiliated Hospital of Nanjing Medical University, No. 300, Guangzhou Road, Nanjing, PR China

²Department of Radiology, Affiliated Hospital of Integrated Traditional Chinese and Western Medicine of Nanjing University of Chinese Medicine, Nanjing, China

³Siemens Healthineers Ltd, Shanghai, China

⁴Department of Thyroid Surgery, The First Affiliated Hospital of Nanjing Medical University, Nanjing, China

Received: 27 June 2023 / Accepted: 3 January 2024

Published online: 18 January 2024

References

1. Moon HJ, Kwak JY, Kim MJ, Son EJ, Kim EK. Can vascularity at power doppler US help predict thyroid malignancy? *Radiology*. 2010;255:260–9.
2. Haugen BR, Alexander EK, Bible KC, et al. 2015 American Thyroid Association Management Guidelines for adult patients with thyroid nodules and differentiated thyroid Cancer: the American Thyroid Association Guidelines Task Force on thyroid nodules and differentiated thyroid Cancer. *Thyroid*. 2016;26:1–133.
3. Roh JL, Park JY, Kim JM, Song CJ. Use of preoperative ultrasonography as guidance for neck dissection in patients with papillary thyroid carcinoma. *J Surg Oncol*. 2009;99:28–31.
4. Kim E, Park JS, Son KR, Kim JH, Jeon SJ, Na DG. Preoperative diagnosis of cervical metastatic lymph nodes in papillary thyroid carcinoma: comparison of ultrasound, computed tomography, and combined ultrasound with computed tomography. *Thyroid*. 2008;18:411–8.
5. Nimmons GL, Funk GF, Graham MM, Pagedar NA. Urinary iodine excretion after contrast computed tomography scan: implications for radioactive iodine use. *JAMA Otolaryngol Head Neck Surg*. 2013;139:479–82.

6. Suh CH, Baek JH, Choi YJ, Lee JH. Performance of CT in the Preoperative Diagnosis of Cervical Lymph Node Metastasis in patients with papillary thyroid Cancer: a systematic review and Meta-analysis. *AJNR Am J Neuroradiol*. 2017;38:154–61.
7. Forghani R. An update on advanced dual-energy CT for head and neck cancer imaging. *Expert Rev Anticancer Ther*. 2019;19:633–44.
8. Forghani R, Srinivasan A, Forghani B. Advanced Tissue Characterization and texture analysis using dual-energy computed Tomography: Horizons and emerging applications. *Neuroimaging Clin N Am*. 2017;27:533–46.
9. Liu X, Ouyang D, Li H, et al. Papillary thyroid cancer: dual-energy spectral CT quantitative parameters for preoperative diagnosis of metastasis to the cervical lymph nodes. *Radiology*. 2015;275:167–76.
10. Vita R, leni A, Tuccari G, Benvenega S. The increasing prevalence of chronic lymphocytic thyroiditis in papillary microcarcinoma. *Rev Endocr Metab Disord*. 2018;19:301–9.
11. Xu S, Huang H, Qian J, et al. Prevalence of Hashimoto Thyroiditis in adults with papillary thyroid Cancer and its Association with Cancer recurrence and outcomes. *JAMA Netw Open*. 2021;4:e2118526.
12. Wang Y, Zheng J, Hu X, et al. A retrospective study of papillary thyroid carcinoma: Hashimoto's thyroiditis as a protective biomarker for lymph node metastasis. *Eur J Surg Oncol*. 2023;49:560–7.
13. Ralli M, Angeletti D, Fiore M, et al. Hashimoto's thyroiditis: an update on pathogenic mechanisms, diagnostic protocols, therapeutic strategies, and potential malignant transformation. *Autoimmun Rev*. 2020;19:102649.
14. Chistiakov DA. Immunogenetics of Hashimoto's thyroiditis. *J Autoimmune Dis*. 2005;2:1.
15. Sahlmann CO, Meller J, Siggelkow H, et al. Patients with autoimmune thyroiditis. Prevalence of benign lymphadenopathy. *Nuklearmedizin*. 2012;51:223–7.
16. Paulson LM, Shindo ML, Schuff KG. Role of chronic lymphocytic thyroiditis in central node metastasis of papillary thyroid carcinoma. *Otolaryngol Head Neck Surg*. 2012;147:444–9.
17. Park JE, Lee JH, Ryu KH, et al. Improved Diagnostic Accuracy using arterial phase CT for lateral cervical lymph node metastasis from papillary thyroid Cancer. *AJNR Am J Neuroradiol*. 2017;38:782–8.
18. Jara SM, Carson KA, Pai SJ, et al. The relationship between chronic lymphocytic thyroiditis and central neck lymph node metastasis in north American patients with papillary thyroid carcinoma. *Surgery*. 2013;154:1272–82.
19. Cunha LL, Morari EC, Guihen AC, et al. Infiltration of a mixture of immune cells may be related to good prognosis in patients with differentiated thyroid carcinoma. *Clin Endocrinol (Oxf)*. 2012;77:918–25.
20. Song E, Jeon MJ, Park S, et al. Influence of coexistent Hashimoto's thyroiditis on the extent of cervical lymph node dissection and prognosis in papillary thyroid carcinoma. *Clin Endocrinol (Oxf)*. 2018;88:123–8.
21. Tawfik AM, Razeq AA, Kerl JM, Nour-Eldin NE, Bauer R, Vogl TJ. Comparison of dual-energy CT-derived iodine content and iodine overlay of normal, inflammatory and metastatic squamous cell carcinoma cervical lymph nodes. *Eur Radiol*. 2014;24:574–80.
22. Tan HL, Nyarko A, Duan SL, et al. Comprehensive analysis of the effect of Hashimoto's thyroiditis on the diagnostic efficacy of preoperative ultrasonography on cervical lymph node lesions in papillary thyroid cancer. *Front Endocrinol (Lausanne)*. 2023;13:987906.
23. Roele ED, Timmer VCML, Vaassen LAA, van Kroonenburgh AMJL, Postma AA. Dual-energy CT in Head and Neck Imaging. *Curr Radiol Rep*. 2017;5:19.
24. Vogl TJ, Schulz B, Bauer RW, Stöver T, Sader R, Tawfik AM. Dual-energy CT applications in head and neck imaging. *AJR Am J Roentgenol*. 2012;199:34–539.
25. Luo YH, Mei XL, Liu QR, et al. Diagnosing cervical lymph node metastasis in oral squamous cell carcinoma based on third-generation dual-source, dual-energy computed tomography. *Eur Radiol*. 2023;33:162–71.
26. Wu YY, Wei C, Wang CB, Li NY, Zhang P, Dong JN. Preoperative prediction of cervical nodal metastasis in papillary thyroid carcinoma: value of quantitative dual-energy CT parameters and qualitative morphologic features. *AJR Am J Roentgenol*. 2021;216:1335–43.
27. He M, Lin C, Yin L, Lin Y, Zhang S, Ma M. Value of dual-energy computed tomography for diagnosing cervical lymph node metastasis in patients with papillary thyroid Cancer. *J Comput Assist Tomogr*. 2019;43:970–5.
28. Smith VA, Sessions RB, Lentsch EJ. Cervical lymph node metastasis and papillary thyroid carcinoma: does the compartment involved affect survival? Experience from the SEER database. *J Surg Oncol*. 2012;106:357–62.

Publisher's Note

Springer Nature remains neutral with regard to jurisdictional claims in published maps and institutional affiliations.